

# Usefulness of a deep-inspiration breath-hold $^{18}\text{F}$ -FDG PET/CT technique in diagnosing liver, bile duct, and pancreas tumors

Shigeki Nagamachi<sup>a</sup>, Hideyuki Wakamatsu<sup>a</sup>, Shogo Kiyohara<sup>a</sup>, Seigo Fujita<sup>a</sup>, Shigemi Futami<sup>a</sup>, Hideo Arita<sup>a</sup>, Ryuichi Nishii<sup>a</sup>, Shozo Tamura<sup>a</sup> and Keiichi Kawai<sup>b</sup>

**Background** The deep-inspiration breath-hold  $^{18}\text{F}$ -fluorodeoxyglucose PET/computed tomography (DIBH  $^{18}\text{F}$ -FDG PET/CT) technique improves the limitations of diagnosing a lesion located in an area influenced by respiratory motion that brings about spatial misregistration caused by respiration between PET and CT. However, its clinical effectiveness with regard to abdominal lesions has not been elucidated. The influence of respiratory motion for calculating the maximal standardized uptake value ( $\text{SUV}_{\text{max}}$ ) and metabolic volume (MV) in DIBH  $^{18}\text{F}$ -FDG PET/CT has not been investigated either.

**Objective** The purpose of this study was to investigate the usefulness of the DIBH  $^{18}\text{F}$ -FDG PET/CT technique in diagnosing liver tumors, bile duct cancers, and pancreas tumors. In addition, we compared the values of  $\text{SUV}_{\text{max}}$  and MV between DIBH and nonbreath-hold (NBH).

**Methods** Forty patients with various abdominal malignancies including liver tumors, bile duct cancers, and pancreas tumors were enrolled. In total, the patients had 47 abdominal lesions. All patients showed a misregistered image in the early whole-body image taken 50 min after intravenous  $^{18}\text{F}$ -FDG infusions. We added the delayed images 40 min after the first image. On the delayed image, we carried out both conventional techniques with normal respiration (NBH) and the DIBH technique. Finally, we compared two kinds of images in each patient. At the same time, we compared both  $\text{SUV}_{\text{max}}$  and MV of cancer obtained by the two kinds of imaging methods.

**Results** In 14 lesions (29.8%), we corrected the anatomical tumor location, from the incorrect to the correct

organ, by the DIBH technique. In 22 lesions (46.8%), we corrected the tumor location within the organ. Consequently, tumor staging also changed in 11 patients (23.4%) after correction by the DIBH technique. Regarding the  $\text{SUV}_{\text{max}}$  value by DIBH, it showed an increase of approximately 15.0–58.6% compared with that measured by NBH. In contrast, the value of MV by DIBH showed a decrease of 20% compared with that measured by NBH.

**Conclusion** The DIBH  $^{18}\text{F}$ -FDG PET/CT technique is feasible for accurate localization when diagnosing of liver tumors, bile duct cancers, and pancreas cancers. The DIBH technique also improves the inaccurate quantification of both  $\text{SUV}_{\text{max}}$  and MV. *Nucl Med Commun* 30:326–332 © 2009 Wolters Kluwer Health | Lippincott Williams & Wilkins.

Nuclear Medicine Communications 2009, 30:326–332

**Keywords:**  $^{18}\text{F}$ -fluorodeoxyglucose PET/computed tomography, bile duct cancer, deep-inspiration breath-hold, liver tumor, pancreas tumor

<sup>a</sup>Department of Radiology, School of Medicine, Miyazaki University, Kihara, Kiyotake, Miyazaki-gun, Miyazaki Prefecture and <sup>b</sup>Faculty of Health Science, School of Medicine, Kanazawa University, Ishikawa Prefecture, Japan

Correspondence to Associate Professor Shigeki Nagamachi, MD, Department of Radiology, School of Medicine, Miyazaki University, 5200 Kihara, Kiyotake, Miyazaki-gun, Miyazaki Prefecture 889-1692, Japan  
Tel: +11 81 985 85 1510 x2244; fax: +11 81 985 85 7172;  
e-mail: snagama@med.miyazaki-u.ac.jp

Received 27 September 2008 Revised 10 November 2008  
Accepted 6 December 2008

## Introduction

The development of combined PET/computed tomography (CT) imaging yields an increased sensitivity and specificity beyond that which either of the two modalities possesses separately and, therefore, provides improved diagnostic accuracy for various cancers [1–4]. As attenuation correction in PET is performed with the use of CT data, accurate spatial registration of PET and CT images sets is required. Therefore, in the interpretation

of PET/CT imaging, the misalignment of structures and lesions owing to respiratory motion is a significant problem [5–7]. It causes not only the misdiagnosis of tumor location but also errors of quantification [6–8]. To overcome this drawback, respiratory gating of PET and CT is available using specific equipment for gating data acquisition [9–12]. However, such equipment requires a long acquisition time for processing the examination and tends to contain a higher degree of noise [9–11].

Recently, the deep-inspiration breath-hold (DIBH) technique has been reported to be likely to overcome these problems. Particularly, it has been validated as a useful technique in the diagnosis of thoracic lesions, such as lung cancer [13–15].

Regarding abdominal lesions, such as liver tumors, the clinical effectiveness of this technique has not been reported despite the possible usefulness of image registration in PET/CT [7]. As the liver has a complicated architecture, such as portal veins or a bile duct system, the correct diagnosis of lesion location is important for determining therapeutic indications.

The effectiveness of DIBH is related to identifying anatomical localizations as well as providing correct quantification. According to a previous report, the maximal standardized uptake values ( $SUV_{max}$ ) by DIBH PET were significantly higher than those by conventional nonbreath-hold (NBH) PET [13,14]. Therefore, by using the DIBH PET/CT technique, we can accurately evaluate lesions close to the diaphragm in quantitative analysis. To the best of our knowledge, the indication of the DIBH technique in the abdominal region has not been confirmed either. Furthermore, a comparative study between NBH and DIBH in the quantification of  $SUV_{max}$  or metabolic volume (MV) has not been conducted previously. The purpose of this study was to investigate the usefulness of the DIBH <sup>18</sup>F-fluorodeoxyglucose PET/CT (DIBH <sup>18</sup>F-FDG PET/CT) technique in diagnosing liver, pancreas or bile duct malignant tumors, and in quantitative analysis.

## Materials and methods

### Patients

Forty patients (27 male, 13 female; average age, 59.2 years; age range, 35–69) with a biopsy-proven diagnosis of cancer confirmed by staff pathologists at the School of Medicine, Miyazaki University, were included. All patients were selected according to the findings of a whole-body image, which showed several misregistrations under NBH conditions. All analyzed lesions comprised 28 liver tumors, 10 bile duct cancers including gall bladder cancer and lymph node metastasis, and nine pancreas cancers. All lesions were solid tumors diagnosed by radiography, CT, and ultrasound. All patients were free from diabetes or chronic obstructive pulmonary disease. They had normal respiratory function. With regard to the tumor maximal diameter, there were no significant differences among abdominal lesions (Table 1).

### Data acquisition and image reconstruction

All PET/CT studies were carried out using an LSO-based whole-body PET/CT scanner (Biograph 16; Siemens Medical Solutions, Knoxville, USA). The CT component of PET/CT corresponds to a 16-slice multidetector-row spiral CT scanner (Sensation 16; Siemens A.G., Forchheim,

**Table 1** Patients' clinical characteristics

	Liver	Bile duct	Pancreas
	(n=22)	(n=9)	(n=9)
Age (years)	68.4 ± 13.5	61.3 ± 10.2	61.3 ± 10.2
Sex (male/female)	16/6	5/4	6/3
Respiratory function			
%FEV1	89.3 ± 7.5	88.2 ± 8.9	78.2 ± 8.9
%VC	92.6 ± 9.2	90.1 ± 8.2	89.6 ± 9.2
Maximal diameter (mm) <sup>a</sup>	25.9 ± 6.9	15.7 ± 7.5	11.7 ± 8.5
COPD	None	None	None
Diabetes mellitus	None	None	None

%FEV1, forced expiratory volume in 1 second; %VC, vital capacity; COPD, chronic obstructive pulmonary disease.

<sup>a</sup>The maximal diameter was calculated as the mean value of lesions.

Germany) with a transverse field of view (FOV) of 500 mm and a spatial resolution greater than 1 mm. The PET component of PET/CT allows only three-dimensional acquisition with a FOV of 700 mm in the transaxial direction and 170 mm in the axial direction. The intrinsic resolution is 4.2-mm full-width-at-half-maximum.

CT images were used for anatomical landmarks. CT-based attenuation correction used 700-mm extended FOV technology. The same clinical reconstruction parameters were used for both NBH PET and DIBH PET images. All PET images were reconstructed using iterative algorithms (Fourier rebinning plus attenuation-weighted ordered-subset expectation maximization, 4 iterations, 8 subset, 5-mm Gaussian filter) with CT-based attenuation correction. The data were reconstructed with a 128 × 128 matrix and 3-mm slice thickness. All PET and CT images were transferred to a dedicated workstation (E.CAM; Siemens Medical Solutions, Irinoi, USA), from which fused PET/CT images were constructed.

We used the following protocol. All patients fasted for at least 5 h before injection of 185 MBq of <sup>18</sup>F-FDG. During the uptake phase of approximately 50 min, the patients remained in a quiet position. The first whole-body image was done in a supine position. The imaging time was 15–18 min for each patient. In addition to the conventional PET/CT examination, all selected patients underwent a DIBH PET/CT scan.

We added a conventional NBH imaging of a spot view after the end of the first whole-body imaging. Just after NBH imaging, we added DIBH spot imaging four times. Each DIBH image datum was acquired under a condition with 30-s breath holding. We completed the final DIBH image by adding each four-DIBH image after the decay correction. All patients provided written informed consent. This study protocol was approved by the Review Board of the Miyazaki University School of Medicine, Japan.

### Image analysis

Image interpretations were performed on a dedicated workstation (ESOFT4.5, Siemens Medical System) that can display three orthogonal planes for CT, PET, and PET/CT fused images (sagittal, coronal, and transaxial) and maximum-intensity projection images. Both NBH PET/CT and DIBH PET/CT images were visually assessed for accuracy of fusion and alignment in separate instances by the same nuclear medicine radiologists, who were unaware of the clinical information. The uptake of  $^{18}\text{F}$ -FDG was considered positive if it was greater than that in the surrounding normal liver tissue. NBH PET/CT images were first interpreted alone and then reevaluated with the addition of DIBH. We made a final diagnosis with an agreement of opinion by three nuclear medicine physicians. A volume of interest was automatically drawn on each lesion with  $^{18}\text{F}$ -FDG uptake on volume images encompassing the entire lesion. The MV of tumor was determined as the lesion with SUV that showed more than 50% of the  $\text{SUV}_{\text{max}}$  value. The  $\text{SUV}_{\text{max}}$ , normalized to the body weight, was recorded for each finding.

Both  $\text{SUV}_{\text{max}}$  and MV values were compared between NBH and DIBH PET/CT. Continuous variables were expressed as the mean  $\pm$  SD. Statistical analyses were conducted by the unpaired Student's *t*-test and the paired *t*-test. A *P* value of less than 0.05 was considered statistically significant.

### Results

Under DIBH conditions, all misregistration uptakes were corrected to the normal anatomical location. They corrected the misregistration uptake from the incorrect organ to the correct organ in 14 of 47 (29.8%) cases, such as from the lung to the liver. Corrections within organs, such as from the upper to the lower area, were observed in 22 of 47 (46.8%) cases. Minor corrections were observed in 11 of 47 (23.4%) cases (Table 2). A minor correction means a correction for various discrepancies between the tumor configuration by CT and the accumulation margin by FDG-PET. The DIBH PET/CT not only allowed a more precise localization of lesion but

**Table 2 Correction of anatomical location**

	<i>n</i>	Major	Moderate	Mild
Liver tumor <sup>a</sup>	28	11	17	0
Pancreas cancer	9	0	2	7
Bile duct cancer <sup>b</sup>	10	3	3	4

Criteria for the correction of tumor's location:

Major: correction from incorrect organ to correct organ.

Mild: adjustment of tumor contour.

Moderate: correction within organ.

<sup>a</sup>Liver tumor included hepatocellular carcinoma, liver metastasis, and cholangiocarcinoma.

<sup>b</sup>Bile duct cancer included extrahepatic bile duct cancer, gall bladder cancer, and lymph node metastases of both.

also accurately corrected the misregistration under NBH conditions in all cases (Figs 1–3).

In quantitative analysis, the mean value of  $\text{SUV}_{\text{max}}$  was statistically higher in the DIBH PET/CT technique than in the NBH study in all evaluated abdominal lesions (Table 3). With regard to MV, the mean value of each region was statistically lower in the DIBH PET/CT technique than in the NBH study (Table 4).

### Discussion

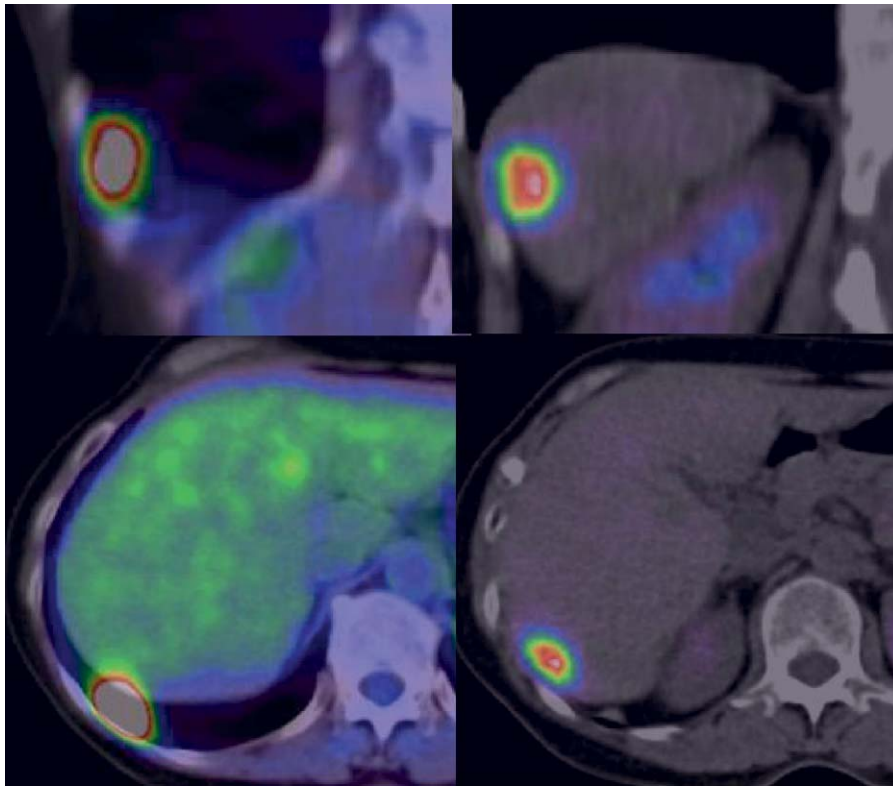
The DIBH technique is usually applied for thoracic lesions because of its effectiveness [13–15]. It is effective for diagnosing the exact location of a lesion and evaluating the number of lesions by avoiding respiratory artifacts. In addition, the method also has the advantage of providing accurate quantitative indices [15].

We confirmed the diagnostic effectiveness of this technique in detecting the accurate anatomical portion of lesions that is located close to the diaphragm, particularly, in the liver. Under the NBH condition, localized uptake was sometimes noted in extrahepatic areas, such as the lower lung. Even when located within the liver, these areas are sometimes overlooked by only plain CT because their density is similar to that of the surrounding tissues. Therefore, incorrectly coregistered localized uptake areas are possibly diagnosed erroneously as tumor location. As a result, tumor staging could be overestimated, and inadequate treatment might be selected. Using the DIBH technique, they were corrected to a true location. In this study, we detected misregistered lesions of liver metastasis and intrahepatic bile duct cancer by NBH. Using the DIBH technique, we could correct the erroneous locations from incorrect to correct organ (39.3%) and from incorrect to correct region within the liver (60.7%). As a result, we could prevent conducting any further examinations unnecessarily, such as thoracic high-resolution CT or repeated respiratory function tests.

In addition, liver nodules are sometimes vaguely visualized by NBH PET/CT because of various physiological uptake of liver tissue. The DIBH technique overcomes the limitations by improving tissue contrast and is helpful for demarcating liver tumors.

Regarding pancreatic tumors, we could obtain relative proper information even when we used the NBH method. No patients showed interorgan misregistration. As the pancreas is located at a relatively greater distance from the diaphragm than the upper liver, the influence of respiratory motion could be small. However, for accurate staging diagnosis, the evaluation of cancer invasion to a surrounding tissue with DIBH technique would be preferable.

Fig. 1



Fifty-four-year-old female with liver metastasis from breast cancer. In the nonbreath-hold (NBH) image (left upper and lower), focal fluorodeoxyglucose uptake appears to show lung metastasis. Using the deep-inspiration breath-hold (DIBH) technique, the liver metastasis was correctly identified (right upper and lower). The maximal standardized uptake value ( $\text{SUV}_{\text{max}}$ ) is 16.54 and the metabolic volume (MV) is 28.45 in NBH, whereas the  $\text{SUV}_{\text{max}}$  is 19.53 and the MV is 28.25 in DIBH.

On the basis of very accurate local coregistration, which makes it possible to do correct attenuation correction and obtain corrected SUV values, increases in the  $\text{SUV}_{\text{max}}$  were observed in most cases [13,15]. The excess rates, which were 20–60%, were comparable with those of previous data with regard to thoracic tumors [10,13,15–17]. Such a phenomenon, including an increased  $\text{SUV}_{\text{max}}$  and an excess rate of approximately 50%, was prominently noted in the liver lesions.

In this mechanism, the lesion of highest SUV is dispersed under the NBH condition with respiratory motion that causes underestimation of the true activity concentration [16–18]. In contrast, under the DIBH condition, the lesion with the highest SUV tends to be fixed, resulting in an increase of the  $\text{SUV}_{\text{max}}$ . As the liver tissue shows physiological uptake in particular, which results in poor delineation, the DIBH technique improves contrast and is helpful for demarcating tumors.

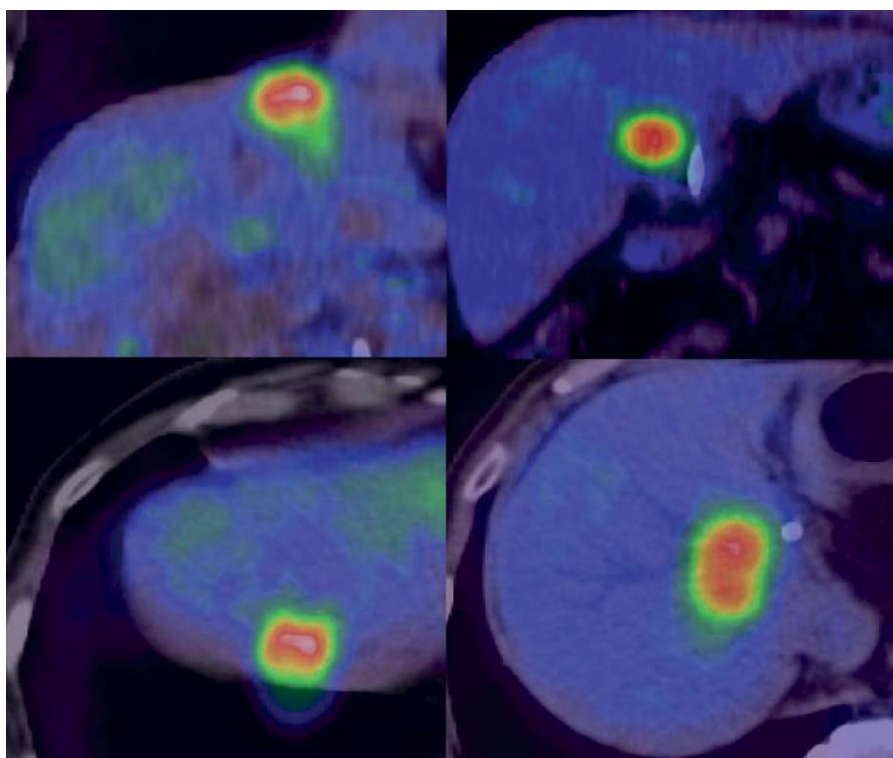
The MV measured by the DIBH technique decreased to about 70% of those measured by NBH in both the liver and the pancreas. In a previous respiration-gated study,

a reduction of about 30% in the total lesion volume was shown [18]. As respiratory motion resulted in the spread of the tumor contour to a larger size than the correct outline, the value of MV seemed to be overestimated. Although the clinical significance of MV has not been determined yet, such an overestimation of the lesion volume may occur. Similar reports have been published in respiratory diffusion-weighted imaging of the liver [19]. The technique is feasible in differentiating malignancy from benign focal liver lesions.

Taking into account those consequences of the DIBH technique, the optimal threshold of  $\text{SUV}_{\text{max}}$  for differentiating between benign and malignant tumors should be reevaluated under controlled respiratory motion. The criteria of the value of the SUV-related index, such as the percentage of increase of a dual-phase study or MV, in differentiation or staging should also be evaluated in the future.

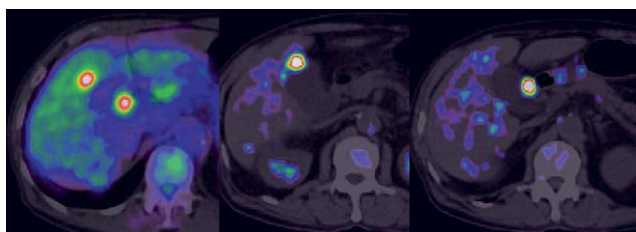
One more implication is the contribution of this technique to the strategy for cancer treatment [13,20]. Recently, radiotherapy has become effective in hepatic

Fig. 2



Sixty-seven-year-old male with cholangiocarcinoma. Under a condition with conventional respiration imaging, the tumor is identified to be partly in the chest (left upper and lower). Under the deep-inspiration breath-hold (DIBH) condition, the tumor is correctly coregistered (right upper and lower). The maximal standardized uptake value ( $SUV_{max}$ ) is 8.5 and the metabolic volume (MV) is 26.8 in nonbreath-hold, whereas the  $SUV_{max}$  is 17.2 and the MV is 16.2 in DIBH.

Fig. 3



Fifty-seven-year-old male with gall bladder (GB) cancer. Under a condition with conventional nonbreath-hold (NBH) imaging, the lesion appears to be multiple hepatic tumors (left). After the correction by deep-inspiration breath-hold (DIBH), cancer is identified in the GB wall and metastatic lymph node is identified in the hepatoduodenal ligament (middle and right). The maximal standardized uptake value ( $SUV_{max}$ ) of the primary lesion is 7.6 and the metabolic volume (MV) is 4.5. In the metastatic lymph node, the  $SUV_{max}$  value is 6.8 and the MV is 3.2 in NBH. In DIBH, the  $SUV_{max}$  of the primary lesion is 8.8 and the MV is 2.7. In the metastatic lymph node, the  $SUV_{max}$  is 8.1 and the MV is 2.2.

or bile duct tumors [20,21]. As tumor location is an important factor for determining the therapeutic method, such as combined radiochemotherapy in the case of bile duct cancer, correct diagnosis using the DIBH technique

Table 3 Comparison of  $SUV_{max}$ 

	<i>n</i>	NBH	DIBH	<i>P</i> value
Liver tumor	28	11.6 ± 3.0	18.4 ± 4.2	0.001
Pancreas cancer	9	10.1 ± 6.4	12.4 ± 5.5	0.024
Bile duct cancer	10	6.0 ± 1.3	6.9 ± 1.5	0.002

DIBH, deep-inspiration breath-hold; NBH, nonbreath-hold;  $SUV_{max}$ , maximal standardized uptake value.

Table 4 Comparison of metabolic volume

	<i>n</i>	NBH (cm <sup>3</sup> )	DIBH (cm <sup>3</sup> )	<i>P</i> value
Liver tumor	28	27.3 ± 12.6	22.7 ± 13.2	0.013
Pancreas cancer	9	16.8 ± 11.1	14.0 ± 11.2	0.044
Bile duct cancer	10	13.9 ± 12.7	11.6 ± 10.7	0.021

DIBH, deep-inspiration breath-hold; NBH, nonbreath-hold.

for anatomical assignment is critical [22]. Moreover, both the extension pattern surrounding the bile duct system and lymph node metastasis also affect the therapeutic strategy [23]. When MV is used as a guide for the radiotherapy planning target volume, a greater dose to the normal tissues may be irradiated under the NBH condition. As liver tissue has limited tolerance to

radiation, inadequate radiation field should be avoided [24]. This conclusion also applies to pancreatic cancer. Major complications, such as radiation-induced liver damage [24] or gastroduodenal ulcers [25–27], must be taken into account. Such undesirable consequences could be avoided by the DIBH technique, and suitable methods, such as intensity-modulated radiation therapy, could be chosen [28].

In addition, as the therapeutic effect cannot always be accurately determined because of the influence of respiratory motion in NBH [29], it is sometimes difficult to select an effective treatment strategy. The FDG-PET/CT technique is now being used to monitor therapeutic effects, such as radio-frequency ablation [30] or the administration of antiangiogenic therapy [31] in liver metastasis. Within the clinical course, these therapies sometimes resulted in unsuccessful treatment or local relapse [30]. Using the DIBH method, we can correctly monitor the therapeutic effects before and after chemotherapy, radiotherapy, and radio-frequency ablation by referring to the change of the corrected SUV<sub>max</sub> or MV. Recently, by the development of radiotherapy treatment methods [32], it has become possible to effectively modify the dose distribution on the basis of the accumulation degree of FDG uptake.

The large drawback of the DIBH technique is that it is not practical for a whole-body scan as a routine examination. The DIBH technique is available within only a one-bed range, which presents limitations in clinical use. If the sensitivity of the PET/CT system is improved and the longitudinal FOVs are increased, it will become a standard method. A future study should include an optimal protocol and appropriate data collection time in many institutions.

## Conclusion

The DIBH <sup>18</sup>F-FDG PET/CT is a feasible technique yielding the precise localization of abdominal malignant lesions located close to the diaphragm and influenced by respiratory motion. In particular, it is useful for diagnosing liver tumor, bile duct cancers, and pancreas cancers. It also provides accurate quantifications for SUV<sub>max</sub> and MV.

## References

- Kim SK, Allen-Auerbach M, Goldin J, Fueger BJ, Dahlbom M, Brown M, *et al.* Accuracy of PET/CT in characterization of solitary pulmonary lesions. *J Nucl Med* 2007; **48**:214–220.
- Halpern BS, Yeom K, Fueger BJ, Lufkin RB, Czernin J, Allen-Auerbach M. Evaluation of suspected local recurrence in head and neck cancer: a comparison between PET and PET/CT for biopsy proven lesions. *Eur J Radiol* 2007; **62**:199–204.
- Mottaghy FM, Sunderkötter C, Schubert R, Wohlfart P, Blumstein NM, Neumaier B, *et al.* Direct comparison of [<sup>18</sup>F] FDG PET/CT with PET alone and with side-by-side PET and CT in patients with malignant melanoma. *Eur J Nucl Med Mol Imaging* 2007; **34**:1355–1364.
- Nehmeh SA, Erdi YE. Respiratory motion in positron emission tomography/computed tomography: a review. *Semin Nucl Med* 2008; **38**:167–176.
- Cohade C, Osman M, Marshall LN, Wahl RN. PET-CT: accuracy of PET and CT spatial registration of lung lesions. *Eur J Nucl Med Imaging* 2003; **30**:721–726.
- Townsend DW. Dual-modality imaging: combining anatomy and function. *J Nucl Med* 2008; **49**:938–955.
- Vogel WV, van Dalen JA, Wiering B, Huisman H, Corstens FH, Ruers TJ, Oyen WJ. Evaluation of image registration in PET/CT of the liver and recommendations for optimized imaging. *J Nucl Med* 2007; **48**:910–919.
- Francis DL, Visvikis D, Costa DC, Arulampalam TH, Townsend C, Luthra SK, *et al.* Potential impact of [<sup>18</sup>F] 3'-deoxy-3'-fluorothymidine versus [<sup>18</sup>F]fluoro-2-deoxy-D-glucose in positron emission tomography for colorectal cancer. *Eur J Nucl Med Imaging* 2003; **30**:344–353.
- Dawood M, Lang N, Jiang X, Schäfers KP. Lung motion correction on respiratory-gated 3-D PET/CT images. *IEEE Trans Med Imaging* 2006; **25**:476–485.
- Larson SM, Nehmeh SA, Erdi YE, Humm JL. PET/CT in non-small-cell lung cancer: value of respiratory-gated PET. *Chang Gung Med J* 2005; **28**:306–314.
- Boucher L, Rodrigue S, Lecomte R, Bénard F. Respiratory gating for 3-dimensional PET of the thorax: feasibility and initial results. *J Nucl Med* 2004; **45**:214–219.
- Hamill JJ, Bosmans G, Dekker A. Respiratory-gated CT as a tool for the simulation of breathing artifacts in PET and PET/CT. *Med Phys* 2008; **35**:576–585.
- Meirelles GSP, Erdi YE, Nehmeh SA, Squire OD, Larson SM, Humm JL, Schöder H. Deep-inspiration breath-hold PET/CT: clinical findings with a new technique for detection and characterization of thoracic lesions. *J Nucl Med* 2007; **48**:712–719.
- Nehmeh SA, Erdi YE, Meirelles GSP, Squire O, Larson SM, Humm JL, Schöder H. Deep-inspiration breath-hold PET/CT of the thorax. *J Nucl Med* 2007; **48**:22–26.
- Kawano T, Ohtake E, Inoue T. Deep-inspiration breath-hold PET/CT of lung cancer: maximum standardized uptake value analysis of 108 patients. *J Nucl Med* 2008; **49**:1223–1231.
- Nehmeh SA, Erdi YE, Ling CC, Rosenzweig KE, Schoder H, Larson SM, *et al.* Effect of respiratory gating on quantifying PET images of lung cancer. *J Nucl Med* 2002; **43**:876–881.
- Nehmeh SA, Erdi YE, Pan T, Pevsner A, Rosenzweig KE, Yorke E, *et al.* Four-dimensional (4D) PET/CT imaging of the thorax. *Med Phys* 2004; **31**:3179–3186.
- Nehmeh SA, Erdi YE, Ling CC, Rosenzweig KE, Squire OD, Braban LE, *et al.* Effect of respiratory gating on reducing lung motion artifacts in PET imaging of lung cancer. *Med Phys* 2002; **29**:366–371.
- Gourtsoyianni S, Papanikolaou N, Yarmenitis S, Maris T, Karantanas A, Gourtsoyiannis N. Respiratory gated diffusion-weighted imaging of the liver: value of apparent diffusion coefficient measurements in the differentiation between most commonly encountered benign and malignant focal liver lesions. *Eur Radiol* 2008; **18**:486–492.
- Zeng ZC, Tang ZY, Fan J, Zhou J, Qin LX, Ye SL, *et al.* Consideration of the role of radiotherapy for unresectable intra-hepatic cholangiocarcinoma: a retrospective analysis of 75 patients. *Cancer J* 2006; **12**:113–122.
- Ben-David MA, Griffith KA, Abu-Isa E, Lawrence TS, Knol J, Zalupski M, *et al.* External-beam radiotherapy for localized extra-hepatic cholangio-carcinoma. *Int J Radiat Oncol Biol Phys* 2006; **66**:772–779.
- Takeuchi S, Saito H, Hokodate H, Yuasa N, Takei T, Takamura A. Criteria for indications for IVR therapy from the standpoint of MDCT and MRI, and technical points. *Japanese J Diagn Imaging* 2006; **26**:585–594.
- Serafini FM, Sachs D, Bloomston M, Carey LC, Karl RC, Murr MM, *et al.* Location, not staging, of cholangiocarcinoma determines the role for adjuvant chemo-radiation therapy. *Am Surg* 2001; **67**:839–843.
- Kim TH, Kim DY, Park JW, Kim SH, Choi JI, Kim HB, *et al.* Dose-volumetric parameters predicting radiation-induced hepatic toxicity in unresectable hepatocellular carcinoma patients treated with three-dimensional conformal radiotherapy. *Int J Radiat Oncol Biol Phys* 2007; **67**:225–231.
- Morganti AG, Valentini V, Macchia G, Mattiucci GC, Costamagna G, Deodato F, *et al.* 5-Fluorouracil-based chemoradiation in unresectable pancreatic carcinoma: phase III dose-escalation study. *Int J Radiat Oncol Biol Phys* 2004; **59**:1454–1460.
- Kawakami H, Uno T, Isobe K, Ueno N, Aruga T, Sudo K, *et al.* Toxicities and effects of involved-field irradiation with concurrent cisplatin for unresectable carcinoma of the pancreas. *Int J Radiat Oncol Biol Phys* 2005; **62**:1357–1362.
- Foo ML, Gunderson LL, Bender CE, Buskirk SJ. External radiation therapy and transcatheter iridium in the treatment of extrahepatic bile duct carcinoma. *Int J Radiat Oncol Biol Phys* 1997; **39**:929–935.

- 28 Milano MT, Chumura SJ, Garofalo MC, Rash C, Roeske JC, Connell PP, *et al.* Intensity-modulated radiotherapy in treatment of pancreatic and bile duct malignancies: toxicity and clinical outcome. *Int J Radiat Oncol Biol Phys* 2004; **59**:445–453.
- 29 Chetty IJ, Fernando S, Kessler ML, McShan DL, Brooks C, Ten Haken RK, Kong FM. Monte Carlo-based lung cancer treatment planning incorporating PET-defined target volumes. *J Appl Clin Med Phys* 2005; **6**:65–76.
- 30 Travaini LL, Trifirò G, Ravasi L, Monfardini L, Della Vigna P, Bonomo G, *et al.* Role of [<sup>18</sup>F]FDG-PET/CT after radiofrequency ablation of liver metastases: preliminary results. *Eur J Nucl Med Mol Imaging* 2008; **35**:1316–1322.
- 31 Scheer MG, Stollman TH, Vogel WV, Boerman OC, Oyen WJ, Ruers TJ. Increased metabolic activity of indolent liver metastases after resection of a primary colorectal tumor. *J Nucl Med* 2008; **49**: 887–891.
- 32 Brunetti J, Caggiano A, Rosenbluth B, Vialotti C. Technical aspects of positron emission tomography/computed tomography fusion planning. *Semin Nucl Med* 2008; **38**:129–136.